J. Fluid Mech. (2007), *vol.* 570, *pp.* 227–252.
doi:10.1017/S0022112006002874 Printed in the United Kingdom

Pressure-dependent viscosity and interfacial instability in coupled ice–sediment flow

By CHRISTIAN SCHOOF

Department of Earth and Ocean Sciences, University of British Columbia,
6339 Stores Road, Vancouver, BC, V6T 1Z4, Canada

(Received 20 July 2005 and in revised form 24 May 2006)

We study an interfacial instability in the coupled flow of ice and subglacial sediment, both modelled as viscous media. Unlike other interfacial instabilities in coupled viscous flows at zero Reynolds number, the mechanism considered here does not rely on buoyancy or the effect of an upper free surface, but on the pressure-dependence of the sediment viscosity. Specifically, the instability relies on sediment rheology being such that, when sediment flows in simple shear, sediment flux increases with compressive normal stress at the ice–sediment interface when the velocity of the interface is kept constant. When ice moves over a shallow bump in the interface, it generates a higher compressive stress on the bump's upstream side than in its lee. If in addition the effective sediment viscosity is low compared with that of ice, interfacial velocity remains approximately constant, and this then implies that more sediment flows into the bump than out of it, causing it to grow. Modelling ice as a Newtonian material, we show that this mechanism works for a wide range of sediment rheologies, including the highly nonlinear shear-thinning ones typically thought most appropriate for the description of 'nearly plastic' sediment. The instabilities predicted are essentially two-dimensional, with infinite transverse wavelength, and a nonlinear model shows that growth is unbounded until cavitation occurs in the lee of evolving bumps on the interface. The instability mechanism does not seem to predict the formation of common glacial landforms, but may explain the formation of water-filled cavities on deformable glacier beds.

1. Introduction

Glaciers and ice sheets are often underlain by deformable sediments known as *till*. Interactions between glacier ice and these sediments can play an important role in glacier sliding (Blankenship *et al.* 1986), in the subglacial drainage of meltwater (Walder & Fowler 1994), and in shaping glacial landscapes. The purpose of this paper is to examine an interfacial instability in the coupled flow of ice and sediment first proposed by Hindmarsh (1998) and Fowler (2000, 2001). Their primary aim was to describe a mechanism for the formation of certain patterned glacial landforms known as drumlins (see figure 1), which Fowler viewed as subglacial analogues of dunes in deserts and on river beds. The underlying mechanism may be of wider interest in the study of complex fluids because it is caused by the viscosity of the modelled subglacial sediment layer being pressure-dependent.

Hindmarsh and Fowler's instability mechanism may be paraphrased as follows: for a certain class of sediment rheologies with pressure-dependent viscosities, sediment flux increases when compressive normal stress at the top of a thin sediment layer increases

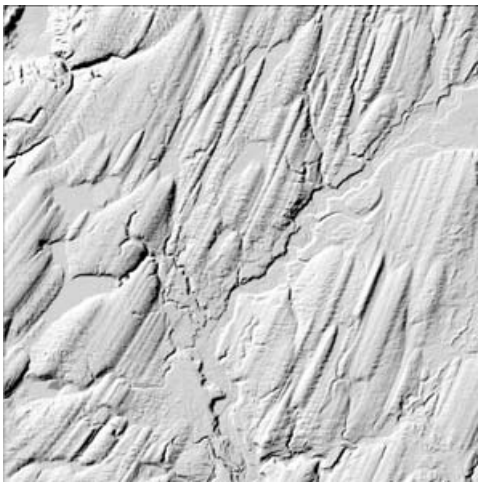

FIGURE 1. Digital elevation model of the Puget Sound drumlin field (Washington State, USA), image courtesy of Ralph Haugerud, US Geological Survey. Shown is a $6 \times 6\,\mathrm{km}^2$ section of the southern Puget Sound, with a quasi-regular pattern of glacial bedforms clearly visible. The typical height of a drumlin in this area is around 15 m. Drumlins form part of a wider spectrum of subglacial bedforms, which also includes transverse Rogen moraine ridges and highly elongated megaflutes (see Aario 1987).

while its surface velocity is kept constant. When ice flows over a shallow bump in the ice–till interface, it exerts higher compressive normal stresses on the upstream side of the bump than on its downstream side. If the viscosity of ice is also much greater than that of till, the till surface velocity remains approximately constant, and combined with the assumed rheological properties of the till, this implies that more sediment flows into the bump than out of it. In turn, this causes the bump to grow. This mechanism differs from those driving better known interfacial instabilities in shearing flows at zero Reynolds number, which usually rely on buoyancy or the presence of an upper free boundary (e.g. Kao 1968; Balmforth, Craster & Toniolo 2003), through its reliance on a pressure-dependent viscosity. Notably, the instability occurs even though the lower fluid (sediment) has a greater density than the upper fluid (ice), and the upper fluid can have infinite thickness.

Hindmarsh and Fowler's analysis was restricted to demonstrating the existence of a linear instability in two dimensions (whereas drumlins are clearly three-dimensional), and they were unable to make statements about the nonlinear evolution of the instability and the shape of the fully evolved interface. The present paper is aimed at filling some of these gaps in their theory. We do not, however, assume that the mechanism being studied is involved in drumlin formation. As we shall see, Hindmarsh and Fowler's theory does not reproduce a number of known features of drumlins and similar subglacial landforms (for instance, their three-dimensional shape), but could instead account for the formation of cavities on deformable glacier beds. These have been observed under the Antarctic sheet (http://www.jpl.nasa.gov/releases/2001/borehole.html), and may play an important role in subglacial drainage and the generation of so-called glacier surges (Fowler 1989; Greenberg & Shyong 1990).

A key assumption in Hindmarsh and Fowler's work is that deformable subglacial sediment can be modelled as an incompressible viscous medium with a pressure-dependent viscosity (strictly, viscosity is assumed to depend on effective pressure,

the difference between confining pressure and pore pressure in the sediment, with the latter being prescribed in the model). The use of viscous rheologies to describe the deformation of till has engendered a heated debate in glaciology because, as granular media, these sediments may be expected to deform plastically (Kamb 1991; Iverson & Iverson 2001; Fowler 2003). Evidence from laboratory ring-shear tests (Iverson *et al.* 1999; Tulaczyk 1999) largely supports the view that tills can be idealized as plastic materials, but also indicates that at least some tills retain a slight dependence of shear stress on strain rate (see also Kamb 2001) and that certain highly nonlinear shear-thinning rheologies are appropriate models for the flow of these tills.

Moreover, as Fowler (2002) points out, laboratory tests fail to reproduce subglacial conditions as larger grains have to be removed from tills prior to testing in ring-shear devices, so this does not yield conclusive evidence as to the behaviour of sediment found at the base of a glacier or ice sheet. Moreover, till shearing in laboratory tests is usually confined to a narrow band in the centre of the sample, while *in situ* samples of subglacial sediments often show evidence of distributed shearing (Boulton & Dobbie 1998). A number of papers (Tulaczyk 1999; Tulaczyk, Kamb & Engelhardt 2000; Iverson & Iverson 2001) have attempted to reconcile this observation with a plastic till rheology; as Fowler (2002) points out, one of them (Iverson & Iverson 2001) explains distributed shear by effectively fashioning a 'viscous' description of till deformation as a result of randomly distributed Coulomb slip events at depth in the till.

Here we persist with Hindmarsh and Fowler's pressure-dependent viscous till, paying attention to highly nonlinear, 'nearly plastic' rheologies. Dell'Isola & Hutter (1998) have developed a more elaborate, thermodynamically motivated description of viscous till deformation than that used by Hindmarsh and Fowler. The difference between the two is primarily that the constitutive variable controlling till viscosity in dell'Isola & Hutter's paper is porosity, not effective pressure. In the Appendix, we sketch how Hindmarsh and Fowler's simpler model can – after some minor alterations – be derived as a special case of dell'Isola & Hutter's in which only small porosity variations are possible (that is, when an appropriate 'compressibility' for the till is small).

2. The model

Subglacial sediments are granular materials which, when not frozen to the base of a glacier or ice sheet, are usually saturated with liquid water as the pore fluid. We follow Hindmarsh (1998) and Fowler (2000, 2001) in assuming that the pore water does not support significant deviatoric stresses, and that the total stress $\boldsymbol{\sigma}$ supported by the till–water mixture can be partitioned between a porewater pressure p_w and an effective stress $\boldsymbol{\sigma}^e$ (see also the Appendix):

$$\sigma_{ij} = \sigma^e_{ij} - p_w\delta_{ij}, \qquad p_e = -\sigma^e_{ii}/3, \tag{2.1}$$

where the effective pressure p_e is the isotropic pressure supported by the till matrix (i.e. the aggregate of till grains), δ_{ij} is the Kronecker delta and the summation convention is applied. We also assume that the till matrix behaves as an incompressible viscous material with constant porosity ϕ. (In the more general framework developed by dell'Isola & Hutter (1998),we are considering the case of a low 'compressibility', see the Appendix). Strain rate $\boldsymbol{D}$ is defined in terms of the velocity field $\boldsymbol{u}$ in the usual way, $D_{ij} = (\partial u_i/\partial x_j + \partial u_j/\partial x_i)/2$, while deviatoric stress is $\tau_{ij} = \sigma^e_{ij} + p_e\delta_{ij}$, and we assume that the constitutive relation for till is of the form

$$\boldsymbol{D} = F(\tau, p_e)\boldsymbol{\tau}/\tau, \tag{2.2}$$

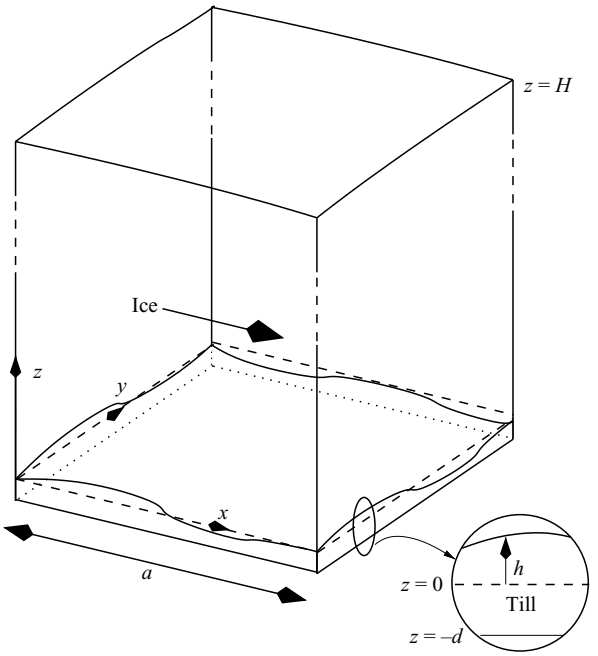

FIGURE 2. Geometry of the problem.

where τ is the second invariant of deviatoric stress, $\tau = (\tau_{ij}\tau_{ij}/2)^{1/2}$. The function F must satisfy $F(0, p_e) = 0$ as well as

$$\frac{\partial F}{\partial \tau} > 0, \qquad \frac{\partial F}{\partial p_e} < 0, \tag{2.3}$$

so till deforms faster under greater applied shear stress and more slowly at higher effective pressure, when till grains are pressed together harder. In addition, we restrict ourselves to $p_e \geqslant 0$ as negative effective pressure corresponds to the disaggregation of the till matrix. The power law (Boulton & Hindmarsh 1987)

$$F(\tau, p_e) = K\frac{\tau^m}{p_e^n} \tag{2.4}$$

will be used as a specific example of a rheology which reproduces the 'nearly plastic' behaviour observed in some ring-shear tests in the parametric limit of large $m \approx n$. What we mean by 'nearly plastic' here and in the remainder of this paper is that shear stress τ in a till sample deforming in simple shear is only weakly dependent on strain rate D, and is related approximately linearly to effective pressure p_e (see also Kamb 2001). Note that the general rheology (2.2) also includes the case of materials which do not deform below a yield stress (such as an effective pressure-dependent Herschel–Bulkley rheology, see e.g. Boulton & Hindmarsh 1987) if one does not insist on strict inequalities in (2.3). We do not, however, pursue this further here.

A Cartesian coordinate system $(x_1, x_2, x_3) = (x, y, z)$ is used with the z-axis pointing vertically upwards. Till is assumed to occupy the space between a fixed flat lower surface $z = -d$ and a mobile ice–sediment interface $z = h(x, y, t)$ (figure 2). Provided the flow of till is slow, conservation of momentum and mass require that on $-d < z < h$

$$\nabla\cdot\boldsymbol{\sigma} - [(1-\phi)\rho_s + \phi\rho_w]g\boldsymbol{k} = \boldsymbol{0}, \qquad \nabla\cdot\boldsymbol{u} = 0, \tag{2.5a, b}$$

where ρ_s is the density of sediment grains, ρ_w the constant density of water, g acceleration due to gravity and $\boldsymbol{k}$ the z-unit vector. Closing the till flow problem requires that water pressure p_w be known. We follow Hindmarsh and Fowler in prescribing a hydrostatic water pressure distribution p_w rather than modelling drainage:

$$p_w = p_c - \rho_w g z, \tag{2.6}$$

where p_c is a constant which can be thought of as the drainage pressure in a pre-existing subglacial drainage system (see e.g. Walder & Fowler 1994; Ng 1998). We assume here for simplicity that the evolution of bed topography does not interfere significantly with the drainage system, allowing p_c to be prescribed; a more elaborate theory would consider p_c as a variable to be modelled separately.

Ice is modelled as a Newtonian medium with viscosity η and density ρ. As in Hindmarsh and Fowler's papers, we assume that the (still unknown) instability length scale is short compared with the thickness H of the ice. Consequently, the ice flow domain is extended to all $z > h$, and we have the usual Stokes equations

$$\eta \nabla^2 \boldsymbol{u} - \nabla p - \rho g \boldsymbol{k} = \boldsymbol{0}, \qquad \nabla \cdot \boldsymbol{u} = 0. \tag{2.7}$$

At the base of the till, we impose no slip,

$$\boldsymbol{u} = \boldsymbol{0} \qquad \text{on } z = -d, \tag{2.8}$$

while we assume that there is no differential motion at the ice–till interface so that velocity, shear and normal stress are continuous:

$$[\boldsymbol{u}]_-^+ = \boldsymbol{0}, \qquad [\boldsymbol{\tau} \cdot \boldsymbol{n} - p\boldsymbol{n}]_-^+ = \boldsymbol{0} \qquad \text{on } z = h. \tag{2.9}$$

$[\cdot]_-^+$ denotes the difference between limiting values taken from above and below, and $\boldsymbol{\tau} \cdot \boldsymbol{n}$ is a contraction, $\tau_{ij} n_j$ in component notation. $\boldsymbol{n}$ is the unit normal to the interface,

$$\boldsymbol{n} = \left[1 + |\nabla_h h|^2\right]^{-1/2} (\boldsymbol{k} - \nabla_h h), \qquad \nabla_h = \boldsymbol{i} \frac{\partial}{\partial x} + \boldsymbol{j} \frac{\partial}{\partial y}, \tag{2.10}$$

and $\boldsymbol{i}$ and $\boldsymbol{j}$ are the unit vectors in the x- and y-directions, respectively. In (2.9), deviatoric stress $\boldsymbol{\tau}$ in the ice ($z > h$) is defined by $\boldsymbol{\tau} = 2\eta \boldsymbol{D}$ as usual. The interface $z = h$ itself satisfies the kinematic boundary condition

$$\frac{\partial h}{\partial t} + u \frac{\partial h}{\partial x} + v \frac{\partial h}{\partial y} = w \qquad \text{on } z = h, \tag{2.11}$$

or, expressed in terms of depth-integrated mass conservation,

$$\frac{\partial h}{\partial t} + \nabla_h \cdot \boldsymbol{q} = 0, \qquad \boldsymbol{q} = \int_{-d}^{h} u \boldsymbol{i} + v \boldsymbol{j} \, \mathrm{d}z. \tag{2.12}$$

In addition, we restrict our domain to (x, y) lying in the square $(0, a) \times (0, a)$ and apply periodic boundary conditions at the edges of the square. Initial conditions are chosen such that the mean of h over the square is zero at $t = 0$, and hence remains at zero for all $t > 0$ by the divergence theorem.

Boundary conditions for the ice flow at $z = \infty$ can be thought of as arising from asymptotic matching between the ice flow problem above as the 'inner problem' (i.e. as a boundary layer near the bed) and an 'outer problem' which describes the bulk flow of the ice sheet (Fowler 1981, 2000) (the horizontal lower boundary of the till implies that the model is appropriate for a continental ice sheet rather than a steep valley glacier). If the function $F(\tau, p_e)$ is not highly nonlinear (specifically, if

the domain of F is all $\tau \geqslant 0$ and $\partial F/\partial \tau$ is not large compared with $F(\tau, p_e)/\tau$), then we can reasonably assume that the outer problem describes a flow in which vertical shearing is dominant, as in the usual lubrication approximation for glacier and ice-sheet flow (Fowler & Larson 1978; Morland & Johnson 1980). This shearing flow imposes a given far-field shear stress $\bar{\tau}$, which we take to be parallel to the x-axis, on the boundary layer, while the pressure field far above the bed becomes hydrostatic. Appropriate boundary conditions are then, as in Hindmarsh and Fowler,

$$\eta\left(\frac{\partial u}{\partial z}+\frac{\partial w}{\partial x}\right)\rightarrow\bar{\tau},\qquad \eta\left(\frac{\partial v}{\partial z}+\frac{\partial w}{\partial y}\right)\rightarrow 0,\qquad p-\rho g(H-z)\rightarrow 0\qquad \text{as } z\rightarrow\infty, \tag{2.13}$$

where $z \rightarrow \infty$ is to be interpreted as z approaching a matching region from below.

In the case of a nearly plastic till, it is appropriate to prescribe a given leading-order velocity on the boundary layer rather than a shear stress, as is discussed in § 7. However, the changes to the model required in that case are minor and we persist with the boundary conditions (2.13) for now.

3. Non-dimensionalization

The model presented in the previous section is a complicated nonlinear moving-boundary problem, and little headway – apart from a brute-force linear stability analysis applied to a basic shearing flow – can be expected without some form of simplification. Hindmarsh (1998) and Fowler (2000, 2001) assume that the flow of subglacial sediment can be described by a thin-film approximation, which they do not, however, carry out consistently. In this section and the next, we demonstrate how Hindmarsh and Fowler's thin-film approximation arises from a perturbation expansion in a small parameter measuring the ratio of till to ice viscosity. This has the advantage of clarifying the assumptions behind the thin film approximation, and of yielding additional simplifications which allow a tractable nonlinear model to be constructed.

We begin by identifying relevant scales and non-dimensionalizing the model. The scalings chosen in this section assume that the till rheology function F is not highly nonlinear (say F given by (2.4) with exponents m and n which are not too large); the rescaling necessary for the more complicated case of 'nearly plastic' rheologies will be considered in § 7. Let $[u]$ and $[w]$ denote scales for horizontal and vertical velocity components, respectively, while $[t]$ is a time scale, $[x]$ a horizontal length scale, $[z]$ a typical depth to which till is deforming significantly, $[h]$ a scale for variations in the elevation of the ice–till interface and $[q]$ a typical till flux. $[N]$ is a deviatoric stress scale, and as the instability mechanism relies on the dependence of till flow on effective pressure, we identify $[N]$ with mean effective pressure at the bed:

$$[N]=\rho g H-p_c. \tag{3.1}$$

Appropriate relations between the remaining scales are

$$[N]=\eta[w]/[x], \tag{3.2}$$

$$[h]/[t]=[u][h]/[x]=[w]=[q]/[x], \tag{3.3}$$

$$[q]=[u][z],\qquad [u]=F(\bar{\tau},[N])[z]. \tag{3.4}$$

$$[z]=d. \tag{3.5}$$

The last relation states that the entire thickness of the sediment layer deforms significantly. This will need to be revisited when we consider highly nonlinear nearly

plastic rheologies in § 7, as the nonlinearity tends to confine till flow to a narrow zone near the ice–till interface. Note that the scale $[h]$ for the amplitude of undulations on the ice–till interface is the same as the deformation depth scale $[z]$ on account of (3.3) and (3.4) – and hence independently of the choice of $[z]$ in (3.5) – while $[t]$ is the advective time scale $[x]/[u]$.

These scales define the dimensionless parameters

$$\nu = \frac{[h]}{[x]}, \qquad \alpha = \frac{(1-\phi)(\rho_s - \rho_w)g[z]}{[N]}, \qquad \beta = \frac{(\rho_w - \rho)g[z]}{[N]}, \qquad \gamma = \frac{[N]}{\bar{\tau}}. \quad (3.6)$$

ν is the aspect ratio of the bed, and the thin-film approximation developed in this paper relies on $\nu \ll 1$. If we define a measure of till viscosity by $\eta_{till} = [z]\bar{\tau}/[u]$, then $\nu = \sqrt{(\eta_{till}[N])/(\eta\bar{\tau})}$. For the case $[N]/\bar{\tau} \sim 1$ considered below, a small aspect ratio ν therefore relies on till being much less viscous than ice. The remaining parameters may be interpreted as follows: α and β measure the relative importance of gravitational terms compared with mean interfacial effective pressure $[N]$ in controlling p_e, and we assume that α and β are positive (i.e. that sediment is denser than water, which is denser than ice). Lastly, γ measures the relative size of normal stress to shear stress at the ice–till interface, which has implications for the flow of till: when $[N]$ and $\bar{\tau}$ are comparable, $\gamma = O(1)$ and till flows in simple shear as a Couette flow at leading order, whereas when $\gamma = O(\nu^{-1})$, pressure gradients appear in the till-flow problem at leading order. In the following, we only consider effective pressure and shear stress of similar magnitude, so $\gamma = O(1)$, as this is the case considered implicitly by Hindmarsh (1998) and Fowler (2000, 2001). The scaling below can also be used to construct a (more complicated) model for the case $\gamma = O(\nu^{-1})$ by analogy with the approach employed in § 4.

Rough estimates for the parameters above can be obtained from values of $[u]$, d, $[N]$, η and $\bar{\tau}$ relevant to parts of ice sheets underlain by deformable beds (such the West Antarctic ice streams, Alley & Bindschadler 2001). As till rheology is poorly constrained, we estimate $[u]$ directly based on ice stream velocities with $[u] = 100$ m $\mathrm{a}^{-1} = 3 \times 10^{-6}\,\mathrm{m\,s^{-1}}$, and put $\bar{\tau} = 5 \times 10^5$ Pa, $[N] = 10^5$ Pa. The estimate for $[N]$ is much less than the hydrostatic ice pressure $\rho g H \approx 10^7$ Pa that one would expect from a 1000 m thick ice sheet, the reason being that significant sediment deformation generally requires high water pressures p_c (cf. Engelhardt & Kamb 1997). We also put $\eta = 2 \times 10^{13}$ Pa s (this can be estimated from Glen's law, Paterson 1994), a deformable sediment thickness of $d = 5$ m, $\rho_s = 2700\,\mathrm{kg\,m^{-3}}$, $\rho_w = 1000\,\mathrm{kg\,m^{-3}}$, $\rho = 900\,\mathrm{kg\,m^{-3}}$ and $\phi = 0.3$, and obtain

$$[x] = \sqrt{\eta[u][h]/[N]} = 55 \text{ m}, \qquad \gamma = 0.5, \qquad \nu = 0.09, \qquad \alpha = 1.2, \qquad \beta = 0.12,$$

and the assumption that $\nu \ll 1$ is apparently justified, while $\alpha = O(1)$. Because the densities of ice and water are similar, $\beta \approx 0.1\alpha$ is typically small, but we retain it here. Note also that the length scale $[x]$ relevant to the model is much less than a typical ice sheet thickness $H \approx 1000$ m, as was assumed previously.

In the till layer $-d < z < h$, we reflect the assumption of a thin film flow by non-dimensionalizing

$$\left.\begin{gathered} h = [h]h^\star, \qquad (x, y, z) = [x](x^\star, y^\star, \nu Z^\star) \qquad (u, v, w) = [u](U^\star, V^\star, \nu W^\star), \\ \boldsymbol{q} = [q]\boldsymbol{q}^\star, \qquad \tau_{xz} = \bar{\tau}\tau^\star_{xz}, \qquad \tau_{yz} = \bar{\tau}\tau^\star_{yz}, \qquad \tau_{xx} = \nu\bar{\tau}\tau^\star_{xx}, \\ \tau_{yy} = \nu\bar{\tau}\tau^\star_{yy}, \qquad \tau_{zz} = \nu\bar{\tau}\tau^\star_{zz}, \qquad \tau_{xy} = \nu\bar{\tau}\tau^\star_{xy}, \qquad p_e = [N]p^\star_e, \\ F(\tau, p_e) = ([u]/[z])F^\star(\tau/\bar{\tau}, p_e/[p_e]), \end{gathered}\right\} \quad (3.7)$$

while in the ice $z > h$, we put

$$(x, y, z) = [x](x^\star, y^\star, z^\star), \qquad (u, v, w) = [u](u^\star, v^\star, w^\star) + \eta^{-1}\bar{\tau}[x]z^\star \boldsymbol{i}, \qquad (3.8a, b)$$

$$p = \rho g(D - z) + \nu^{-1}[N]p^\star. \qquad (3.8c)$$

Note that the same scaling for horizontal coordinates and velocity components is used for the till and ice flows, whereas the scalings for vertical coordinates and velocity components differ by a factor of ν. To avoid confusion, we will use the variables $Z^\star$ and $(U^\star, V^\star, W^\star)$ only to describe vertical position and velocity in the till layer, while $z^\star$ and $\boldsymbol{u}^\star = (u^\star, v^\star, w^\star)$ will be reserved for the ice flow domain. Similarly, $\tau^\star_{xz}$, $\tau^\star_{xy}$ etc. will be used only to describe stress components in the till.

3.1. *Scaled equations*

We do not reproduce the full scaled versions of (2.1)–(2.13), which can easily be obtained by substitution from (3.7) and (3.8). Instead we list the relevant scaled equations with 'small' terms (of the order indicated on the right-hand side) omitted. We also omit the asterisks on the dimensionless variables to simplify our notation.

The scaled momentum conservation equations for the till then take the usual form for a thin-film flow:

$$\frac{\partial \tau_{xz}}{\partial Z} - \nu\gamma\frac{\partial p_e}{\partial x} = O(\nu^2), \quad \frac{\partial \tau_{yz}}{\partial Z} - \nu\gamma\frac{\partial p_e}{\partial y} = O(\nu^2), \quad \frac{\partial p_e}{\partial Z} + \alpha = O(\nu\gamma^{-1}), \qquad (3.9)$$

on $-1 < Z < h$, where

$$F(\tau, p_e)\frac{\tau_{xz}}{\tau} = \frac{\partial U}{\partial Z} + O(\nu^2), \quad F(\tau, p_e)\frac{\tau_{yz}}{\tau} = \frac{\partial V}{\partial Z} + O(\nu^2), \quad \tau^2 = \tau_{xz}^2 + \tau_{yz}^2 + O(\nu^2). \qquad (3.10)$$

We will only require mass conservation for till in its depth-integrated form, which reads

$$\frac{\partial h}{\partial t} + \nabla_h \cdot \boldsymbol{q} = 0, \qquad \boldsymbol{q} = \int_{-1}^{h} U\boldsymbol{i} + V\boldsymbol{j}\,\mathrm{d}Z. \qquad (3.11)$$

Field equations for the ice are of the usual Stokes flow form

$$\nabla^2\boldsymbol{u} - \nabla p = \boldsymbol{0}, \qquad \nabla\cdot\boldsymbol{u} = 0 \qquad \text{on } z > 0. \qquad (3.12)$$

The no-slip conditions at the base of the till $Z = -1$ are unchanged

$$U = V = 0, \qquad (3.13)$$

while velocity and stress continuity at the ice–till interface $z = \nu h$, $Z = h$ leads to

$$u = U, \qquad v = V, \qquad w = \nu\left(\frac{\partial h}{\partial t} + u\frac{\partial h}{\partial x} + v\frac{\partial h}{\partial y}\right), \qquad (3.14a\text{–}c)$$

$$\frac{\partial u}{\partial z} - \frac{\partial w}{\partial x} - \nu\frac{\partial h}{\partial y}\left(\frac{\partial u}{\partial y} - \frac{\partial v}{\partial x}\right) - \nu\frac{\partial h}{\partial x}\left(2\frac{\partial u}{\partial x} - p\right) = \nu\gamma^{-1}(\tau_{xz} - 1) + O(\nu^2, \nu^2\gamma^{-1}), \qquad (3.15)$$

$$\frac{\partial v}{\partial z} - \frac{\partial w}{\partial y} - \nu\frac{\partial h}{\partial x}\left(\frac{\partial v}{\partial x} - \frac{\partial u}{\partial y}\right) - \nu\frac{\partial h}{\partial y}\left(2\frac{\partial v}{\partial y} - p\right) = \nu\gamma^{-1}\tau_{yz} + O(\nu^2, \nu^2\gamma^{-1}), \qquad (3.16)$$

$$2\frac{\partial w}{\partial z} - p + \nu\frac{\partial h}{\partial y}\left(\frac{\partial v}{\partial z} - \frac{\partial w}{\partial y}\right) - \nu\frac{\partial h}{\partial x}\left(\frac{\partial u}{\partial z} - \frac{\partial w}{\partial x}\right) = -\nu(p_e - 1 - \beta h) + O(\nu^2\gamma^{-1}), \qquad (3.17)$$

and boundary conditions at $z=\infty$ are simply

$$\frac{\partial u}{\partial z}+\frac{\partial w}{\partial x}\to 0, \qquad \frac{\partial v}{\partial z}+\frac{\partial w}{\partial y}\to 0, \qquad p\to 0. \tag{3.18}$$

4. Perturbation expansion

In the remainder of this paper, we exploit the smallness of the aspect ratio parameter ν, and treat the case $\gamma=O(1)$. Dependent variables are expanded as

$$\boldsymbol{u}\sim \boldsymbol{u}^{(0)}+\nu\boldsymbol{u}^{(1)}+O(\nu^2), \qquad p\sim p^{(0)}+\nu p^{(1)}+O(\nu^2) \qquad \text{etc.} \tag{4.1}$$

As pointed out above, we have scaled the vertical (z-) coordinate differently in the ice and till flow domains in (3.7) and (3.8). The boundary conditions for the ice-flow at $z=\nu h$ are expanded in a Taylor series about $z=0$, allowing the ice-flow problem to be considered on the simpler half-space domain $z>0$, while no such expansion is carried out in the coordinate Z.

4.1. *Leading-order ice flow*

The leading-order ice-flow problem obtained from (3.12), (3.14*c*), (3.15), (3.16) and (3.18) takes the form of the homogeneous Stokes equations posed on the half-space $z>0$ with homogeneous Neumann-type boundary conditions in the horizontal velocity components $(u^{(0)}, v^{(0)})$ and homogeneous Dirichlet conditions in pressure $p^{(0)}$ and vertical velocity $w^{(0)}$. Hence we obtain the trivial plug-flow solution

$$\big(u^{(0)}, v^{(0)}\big)\equiv \bar{\boldsymbol{U}}, \qquad w^{(0)}\equiv p^{(0)}\equiv 0, \tag{4.2}$$

where the two-dimensional velocity vector $\bar{\boldsymbol{U}}(t)$ is independent of position (but otherwise unconstrained as yet). This is analogous to the sliding velocity in classical hard-bed sliding with small bed slopes, where the leading-order velocity field in the basal boundary layer is also a plug-flow (Fowler 1981). As we shall see shortly, the plug-flow velocity $\bar{\boldsymbol{U}}$ is determined through the till-flow problem by a simple force balance argument. Importantly, asymptotic matching with the outer flow problem for the glacier or ice sheet leads then to the imposition of a definite 'sliding' velocity $\bar{\boldsymbol{U}}$ at the lower boundary of the outer flow, as the shearing component in (3.8*c*) is small compared with the $\boldsymbol{u}^{\star}$ term (cf. Fowler 1981, see also § 7). Physically, we may ascribe the plug-flow nature of the ice flow to the high viscosity of ice compared with till implicit in $\nu\ll 1$.

4.2. *Till flux and till surface velocity*

The ice velocity $\bar{\boldsymbol{U}}$ as well as the till flux $\boldsymbol{q}^{(0)}$ are determined by the leading-order till-deformation problem obtained from (3.9), (3.10) and (3.13). This leading-order problem describes a simple shearing flow with no-slip boundary conditions on $Z=-1$. For simplicity of notation, we define an interfacial effective pressure N and a two-dimensional basal shear stress vector $\boldsymbol{\tau}_b$ as

$$N=p_e^{(0)}\big|_{Z=h^{(0)}}, \qquad \boldsymbol{\tau}_b=\big(\tau_{xz}^{(0)}\boldsymbol{i}+\tau_{yz}^{(0)}\boldsymbol{j}\big)\big|_{Z=h^{(0)}}. \tag{4.3}$$

If we temporarily omit the explicit dependence of U and V on x, y and t, then integrating (3.9) and (3.10) at leading order gives

$$\big(U^{(0)}(Z), V^{(0)}(Z)\big)=\frac{\boldsymbol{\tau}_b}{\tau_b}\int_{-1}^{Z} F\big(\tau_b, N+\alpha\big(h^{(0)}-Z'\big)\big)\,\mathrm{d}Z', \tag{4.4}$$

where $\tau_b = |\boldsymbol{\tau}_b|$ is the usual Euclidean norm of $\boldsymbol{\tau}_b$. Using (3.11) and (3.14), integration of the till-flow problem then yields till flux $\boldsymbol{q}^{(0)}$ and sliding velocity $\bar{\boldsymbol{U}}$ as functions of $\boldsymbol{\tau}_b$, N and $h^{(0)}$:

$$\left.\begin{aligned} &\bar{\boldsymbol{U}} = u_b\big(\tau_b, N, h^{(0)}\big)\boldsymbol{\tau}_b/\tau_b, \\ &u_b\big(\tau_b, N, h^{(0)}\big) := \int_{-1}^{h^{(0)}} F\big(\tau_b, N+\alpha\big(h^{(0)}-Z\big)\big)\,\mathrm{d}Z = \int_0^{h^{(0)}+1} F\big(\tau_b, N+\alpha\xi\big)\,\mathrm{d}\xi, \end{aligned}\right\} \tag{4.5}$$

$$\left.\begin{aligned} &\boldsymbol{q}^{(0)} = q_b\big(\tau_b, N, h^{(0)}\big)\boldsymbol{\tau}_b/\tau_b, \\ &q_b\big(\tau_b, N, h^{(0)}\big) := \int_{-1}^{h^{(0)}}\int_{-1}^{Z} F\big(\tau_b, N+\alpha\big(h^{(0)}-Z'\big)\big)\,\mathrm{d}Z'\,\mathrm{d}Z \\ &\qquad = \int_0^{h^{(0)}+1} F\big(\tau_b, N+\alpha\xi\big)\xi\,\mathrm{d}\xi, \end{aligned}\right\} \tag{4.6}$$

where $\xi = h^{(0)} - Z$, and we have made use of the identity $\int_b^c \int_b^z f(z')\,\mathrm{d}z'\,\mathrm{d}z = \int_b^c (c-z) f(z)\,\mathrm{d}z$. With the constraints (2.3) on sediment rheology, we obtain the intuitively obvious observations that till flux q_b and surface velocity u_b increase with till thickness $h^{(0)}$ and shear stress τ_b, while they decrease with effective pressure N.

An alternative form of (4.5) and (4.6) will become useful later. As $F(\tau, p_e)$ is a monotonically increasing function of τ, we can invert the relation $\bar{U} = u_b(\tau_b, N, h^{(0)}) = \int_0^{1+h^{(0)}} F(\tau_b, N+\alpha\xi)\,\mathrm{d}\xi$ to find τ_b as a function of $\bar{U} = |\bar{\boldsymbol{U}}|$, N and $h^{(0)}$. Hence we can write $\tau_b = \tau(\bar{U}, N, h^{(0)})$, and (4.5) becomes

$$\boldsymbol{\tau}_b = \tau\big(\bar{U}, N, h^{(0)}\big)\bar{\boldsymbol{U}}/\bar{U}. \tag{4.7}$$

Consequently, shear stress at the ice–till interface is determined by sediment thickness, effective pressure and the plug-flow velocity $\bar{\boldsymbol{U}}$, and is always parallel to the direction of $\bar{\boldsymbol{U}}$ (which is constant in space). Likewise, sediment flux takes the form

$$\boldsymbol{q}^{(0)} = Q\big(\bar{U}, N, h^{(0)}\big)\bar{\boldsymbol{U}}/\bar{U}, \tag{4.8}$$

where the function Q arises from substituting for τ_b in (4.6).

Ultimately, we wish to find the till flux $\boldsymbol{q}^{(0)}(x, y, t)$ which corresponds to a given bed topography $h^{(0)}(x, y, t)$ in order to solve the evolution equation

$$\frac{\partial h^{(0)}}{\partial t} + \nabla_h \cdot \boldsymbol{q}^{(0)} = 0. \tag{4.9}$$

We must therefore determine the interfacial effective pressure $N(x, y, t)$ and plug-flow velocity $\bar{\boldsymbol{U}}(t)$ which result from ice flow over that topography. Importantly, N does not depend on $h^{(0)}$ and its derivatives locally, but must be found by solving for the first-order correction to the ice-flow problem, as must $\bar{\boldsymbol{U}}$. As we shall see later, this can be used to turn the problem into one of integro-differential type.

4.3. *Spatial variations in basal normal stress and shear stress: the ice-flow correction problem*

From (3.12), (3.14*c*), (3.15), (3.16), (3.17) and (3.18) as well as (4.9) and the solution for $\boldsymbol{u}^{(0)}$ above, the $O(\nu)$ ice-flow problem satisfies the following equations:

$$\nabla^2 \boldsymbol{u}^{(1)} - \nabla p^{(1)} = \boldsymbol{0}, \qquad \nabla \cdot \boldsymbol{u}^{(1)} = 0 \qquad \text{on } z > 0 \tag{4.10a, b}$$

$$N = p^{(1)} - 2\frac{\partial w^{(1)}}{\partial z} + \beta h^{(0)} + 1 \qquad \text{on } z = 0, \tag{4.11}$$

$$\boldsymbol{\tau}_b = \boldsymbol{i} + \gamma\left(\frac{\partial u^{(1)}}{\partial z} + \frac{\partial w^{(1)}}{\partial x}, \frac{\partial v^{(1)}}{\partial z} + \frac{\partial w^{(1)}}{\partial y}, 0\right) \qquad \text{on } z = 0, \tag{4.12}$$

$$w^{(1)} = \bar{\boldsymbol{U}} \cdot \nabla_h h^{(0)} - \nabla_h \cdot \boldsymbol{q}^{(0)} \qquad \text{on } z = 0 \tag{4.13}$$

$$\frac{\partial u^{(1)}}{\partial z} + \frac{\partial w^{(1)}}{\partial x} \to 0, \qquad \frac{\partial v^{(1)}}{\partial z} + \frac{\partial w^{(1)}}{\partial y} \to 0, \qquad p^{(1)} \to 0 \qquad \text{as } z \to \infty, \tag{4.14}$$

which may be seen as analogues of the equations decribing velocity and pressure perturbations introduced into basal ice by flow over small-slope undeformable bed topography in classical glacier sliding theory (Nye 1969; Kamb 1970; Fowler 1981). Here, (4.10) are the usual Stokes equations, while (4.13) describes the effect of an uneven evolving bed topography on the velocity field in the ice, which is crucial in causing Hindmarsh and Fowler's instability. Equations (4.12) and (4.11) show that $\boldsymbol{\tau}_b$ and N arise naturally as boundary values of shear stress and normal stress at $O(\nu)$ in the ice flow problem.

Using the fact that $\bar{\boldsymbol{U}}(t)$ does not depend on position, we can simplify the problem further. Integrating (4.10*a*) over the cuboid $(0, a) \times (0, a) \times (0, R)$ and applying the divergence theorem while passing to the limit $R \to \infty$, we arrive at the obvious conclusion that the mean of basal shear stress $\boldsymbol{\tau}_b$ over the ice–till interface must be the dimensionless driving stress $\boldsymbol{i}$ (cf. Schoof 2002, p. 117), while the mean of scaled effective pressure N is unity. Hence, using (4.7), we obtain the solvability conditions

$$\frac{\bar{\boldsymbol{U}}}{a^2 \bar{U}} \int_0^a \int_0^a \tau(\bar{U}, N, h^{(0)})\, \mathrm{d}x\, \mathrm{d}y = \boldsymbol{i}, \qquad \frac{1}{a^2} \int_0^a \int_0^a N\, \mathrm{d}x\, \mathrm{d}y = 1. \tag{4.15a, b}$$

The obvious conclusion from (4.15*a*) is that the sliding velocity $\bar{\boldsymbol{U}}$ is always parallel to the direction of the driving stress (the x-direction). From (4.5) and (4.6) it then follows that the y-components of shear stress $\boldsymbol{\tau}_b$ and hence of till flux $\boldsymbol{q}^{(0)}$ also vanish, so $\bar{\boldsymbol{U}} = \bar{U}\boldsymbol{i}$, $\boldsymbol{\tau}_b = \tau_b \boldsymbol{i}$ and $\boldsymbol{q}^{(0)} = q^{(0)}\boldsymbol{i}$. As we shall see in § 6, the role of the second condition (4.15*b*) is to fix the mean sediment flux at the bed.

These results allow the ice-flow model to be simplified by replacing boundary conditions (4.13) and (4.12) as well as the till evolution equation (4.9) by

$$w^{(1)} = \bar{U}\frac{\partial h^{(0)}}{\partial x} - \frac{\partial q^{(0)}}{\partial x} \qquad \text{on } z = 0, \tag{4.16}$$

$$\tau_b = 1 + \gamma\left(\frac{\partial u^{(1)}}{\partial z} + \frac{\partial w^{(1)}}{\partial x}\right), \qquad \frac{\partial v^{(1)}}{\partial z} + \frac{\partial w^{(1)}}{\partial y} = 0 \qquad \text{on } z = 0 \tag{4.17}$$

$$\frac{\partial h^{(0)}}{\partial t} + \frac{\partial q^{(0)}}{\partial x} = 0, \tag{4.18}$$

respectively, where $\tau_b = \tau(\bar{U}, N, h^{(0)})$, $q = Q(\bar{U}, N, h^{(0)})$, and $\bar{U}(t)$ is determined by (4.15*a*):

$$\int_0^a \int_0^a \tau\left(\bar{U}, N, h^{(0)}\right) - 1\, \mathrm{d}x\, \mathrm{d}y = 0. \tag{4.19}$$

Note that there are four scalar boundary conditions in (4.11), (4.16) and (4.17) to be satisfied at the bed, when ordinarily we would expect only three for a three-dimensional Stokes flow problem. The additional boundary condition arises because N is not known *a priori* even if we consider a fixed t and $h^{(0)}(x, t)$ is given, but must be found as part of the solution. Specifically, (4.16) and (4.17) are nonlinear boundary conditions which link the vertical velocity component $w^{(1)}$ and shear stress term

$\partial u^{(1)}/\partial z + \partial w^{(1)}/\partial x$ at the bed to the boundary value $p^{(1)} - 2\partial w^{(1)}/\partial z$ of normal stress, and hence to N, through the till deformation functions $\tau(\bar{U}, N, h)$ and $Q(\bar{U}, N, h)$. We can therefore think of the boundary-value problem consisting of (4.10), (4.11), (4.14) and (4.16), (4.17) as determining N in terms of $h^{(0)}$, while (4.19) serves to determine the spatially constant term $\bar{U}$. Taken together, these allow N and $\bar{U}$ to be found for a given bed topography $h^{(0)}$, and the evolution equation (4.18) to be solved using $q^{(0)} = Q(\bar{U}, N, h^{(0)})$. (Note that the Neumann boundary conditions on $u^{(1)}$ and $v^{(1)}$ imply that the horizontal first-order velocity components are defined only up to an additive constant, which does, however, not affect the determination of effective pressure N described above. In order to obtain a unique first-order velocity field $\boldsymbol{u}^{(1)}$ it suffices to require in addition that, for instance, the mean of $u^{(1)}$ and $v^{(1)}$ over the bed be zero.)

An important difference between the present model and classical glacier sliding theory – apart from the fact that the bed is able to evolve – is that the force balance relation (4.19) does not contain the 'upstream component' of normal stress at the bed, which is usually taken to be the dominant term in force balance for an undeformable bed (Nye 1969; Fowler 1981). In the context of the present model, this term, which is associated with form drag, only becomes important when $\gamma = O(\nu^{-1})$, a case not considered here.

Apart from the nonlinearity retained in our model through the functions Q and τ, the main difference between the reduced model constructed in this section and the linearized models of Hindmarsh and Fowler lies in our recognition that the ice flow is, at leading-order, a plug flow, while Hindmarsh and Fowler allow for leading-order variations in ice velocity at the interface (which we expect to be small on account of (3.14*c*), (3.15) and (3.16)). Ignoring these velocity variations simplifies the subsequent analysis considerably.

5. Linear stability analysis

We examine the stability of the flat interface $h^{(0)} \equiv 0$ in the model given by equations (4.10), (4.13), (4.14) and (4.16)–(4.19). This will allow us to verify that our systematically reduced model captures Hindmarsh's (1998) and Fowler's (2000, 2001) instability mechanism, and to shed further light on what causes the instability.

Consider small perturbations about a basic laminar shearing flow:

$$h^{(0)} = \varepsilon h'(x, y, t), \qquad \boldsymbol{u}^{(1)} = \varepsilon \boldsymbol{u}'(x, y, z, t), \qquad p^{(1)} = \varepsilon p'(x, y, z, t),$$

$$N = 1 + \varepsilon N'(x, y, t), \qquad \bar{U} = \bar{U}_0 + \varepsilon^2 \bar{U}'(t),$$

where $\varepsilon \ll 1$ measures the size of the perturbation, and $\bar{U}_0 = \int_0^1 F(1, 1+\alpha\xi)\,\mathrm{d}\xi$ is the surface velocity of the till in the basic shearing-flow solution. The perturbation to $\bar{U}_0$ is of $O(\varepsilon^2)$ because $\bar{U}$ is independent of position while h' and N' have zero spatial mean (formally, this is justified by linearizing the constraint (4.19), cf. Schoof 2002, p. 121). The relationships $q = Q(\bar{U}, N, h)$ and $\tau_b = \tau(\bar{U}, N, h)$ are linearized as

$$q = Q(\bar{U}_0, 1, 0) + \varepsilon Q_N N' + \varepsilon Q_h h' + O(\varepsilon^2), \qquad \tau_b = 1 + \varepsilon \tau_N N' + \varepsilon \tau_h h' + O(\varepsilon^2), \quad (5.1)$$

where $Q_N = \partial Q/\partial N|_{(\bar{U}_0,1,0)}$, $Q_h = \partial Q/\partial h|_{(\bar{U}_0,1,0)}$, and similarly for τ_N and τ_h.

By looking for Fourier mode solutions of the form $h' = \hat{h}\exp(\mathrm{i}k_x x + \mathrm{i}k_y y + \sigma t)$, we obtain an algebraic eigenvalue problem for σ very similar to that in Fowler (2000, 2001). The straightforward solution procedure is analogous to that used by Fowler (see also Schoof 2002, §§ 5.3–5.4), and allows the dispersion relation for the linearized

problem to be calculated as

$$\sigma = -\mathrm{i}k_x \frac{Q_h + \beta Q_N + 2\mathrm{i}k_x k Q_N \bar{U}_0}{1 + 2\mathrm{i}k_x k Q_N}, \tag{5.2}$$

where $k = \sqrt{k_x^2 + k_y^2}$. The corresponding growth rate is

$$\mathrm{Re}(\sigma) = \frac{2Q_N(\bar{U}_0 - Q_s - \beta Q_N)k_x^2 k}{1 + 4Q_N^2 k_x^2 k^2}, \tag{5.3}$$

and we see immediately that the bed is neutrally stable with $\mathrm{Re}(\sigma) = 0$ if $Q_N = 0$, i.e. if till flux is independent of effective pressure. As mentioned earlier, the absence of an upper free boundary to the ice flow domain implies that the instability mechanism relies entirely on the dependence of till rheology, and hence of till flux, on effective pressure (see also Fowler 2000, 2001).

Specifically, instability ($\mathrm{Re}(\sigma) > 0$) requires that

$$Q_N(\bar{U}_0 - Q_h - \beta Q_N) > 0. \tag{5.4}$$

If this condition is satisfied, then the fastest growing Fourier mode has a wavevector of the form $(k_x, k_y)_{max} = (\pm[\sqrt{3}/(2|Q_N|)]^{1/2}, 0)$, which has zero transverse component, corresponding to infinite transverse wavelength. This suggests that if the instability occurs, then it causes transverse roll waves at the ice–till interface rather than three-dimensional shapes like drumlins. Physically, this may be attributed to there being no transverse component of till flux at leading order, which in turn results from the plug-flow nature of the ice flow and hence from the high viscosity of ice compared with till. In addition, (5.3) indicates that the linearized problem is well-posed, with $\mathrm{Re}(\sigma) \sim k^{-1}$ as $k \to \infty$.

Before we investigate the instability criterion (5.4) further, we point out that when restricted to the two-dimensional case $k_y = 0$, the growth rate calculated in (5.3) can be shown to be a dimensionless version of the growth rate in equation (5.2) in Fowler (2000), and our reduced model therefore captures the same instability mechanism as Fowler's model.

5.1. *The instability criterion*

For a better insight into the physical instability mechanism, we consider under what conditions on the function $F(\tau, p_e)$ and the parameter β the instability criterion (5.4) is satisfied. Using $Q(\bar{U}, N, h) = q_b(\tau_b, N, h)$ where $\bar{U} = u_b(\tau_b, N, h)$, we can relate derivatives of $Q(\bar{U}, N, h)$ to derivatives of $u_b(\tau_b, N, h)$ and $q_b(\tau_b, N, h)$ by using the chain rule:

$$\frac{\partial Q}{\partial h} = \frac{\partial q_b}{\partial h} - \frac{\partial q_b}{\partial \tau_b}\frac{\partial u_b}{\partial h}\Big/\frac{\partial u_b}{\partial \tau_b}, \qquad \frac{\partial Q}{\partial N} = \frac{\partial q_b}{\partial N} - \frac{\partial q_b}{\partial \tau_b}\frac{\partial u_b}{\partial N}\Big/\frac{\partial u_b}{\partial \tau_b}. \tag{5.5a, b}$$

As discussed in § 4.2, till flux $q_b(\tau_b, N, h)$ and till velocity $u_b(\tau_b, N, h)$ increase with τ_b and h while they decrease with N. Therefore the second term on the right-hand side of (5.5*a*) is negative and $\partial Q/\partial h < \partial q_b/\partial h$. The basic solution of a simple shearing flow corresponds to $\tau_b = 1$, $N = 1$ and $h = 0$, and for these values, $\partial q_b/\partial h = F(1, 1+\alpha)$ follows from the definition of till flux in (4.6). Hence $Q_h < F(1, 1+\alpha)$ and

$$\bar{U}_0 - Q_h > \int_0^1 F(1, 1 + \alpha\xi)\,\mathrm{d}\xi - F(1, 1 + \alpha) > 0, \tag{5.6}$$

because $\alpha > 0$ and F is strictly decreasing in its second argument. Since $\beta > 0$, the instability criterion (5.4) is therefore satisfied if and only if

$$Q_N > 0, \qquad \beta < \frac{\bar{U}_0 - Q_h}{Q_N}. \tag{5.7}$$

Assuming for the moment that the difference between the densities ρ_w of water and ρ of ice is small enough for $\beta = (\rho_w - \rho)g[z]/[N]$ to be negligibly small, we see that the instability essentially requires $Q_N > 0$. As indicated in § 1, till flux must increase with effective pressure when the sliding velocity is held constant.

The instability therefore functions as indicated in § 1: the flow of ice over a bump on the bed causes higher compressive normal stresses, and hence higher interfacial effective pressures N, on the upstream side of the bump than on the downstream side. Meanwhile, the plug flow nature of the ice flow at leading order implies that the surface velocity of the till remains approximately constant on both sides of the bump. If till rheology is such that till flux increases at constant till surface velocity when interfacial effective pressure is increased, then the higher normal stresses on the upstream side than on the downstream side of a bed bump cause a greater till flux into the bump than out of it, and the bump grows.

Intuitively, one would associate an increase in effective pressure not with an increase in till flux – which the instability demands – but with a decrease, and this is certainly true at constant shear stress ($\partial q_b/\partial N < 0$ as discussed above). Till flux can increase with effective pressure only because the stiffening of till at increased effective pressure also requires an increased shear stress to keep till surface velocity constant – this is expressed by the second (positive) term on the right-hand side of (5.5*b*), while the direct effect of increased effective pressure on till flux is represented by the first (negative) term. Which of these two effects dominates depends on the particular rheological model for till, i.e. on the function F.

Using (5.5*b*) and defining $F_\tau = \partial F/\partial \tau$, $F_{p_e} = \partial F/\partial p_e$, we find

$$Q_N = \int_0^1 \xi F_{p_e}(1, 1+\alpha\xi)\,\mathrm{d}\xi - \frac{\displaystyle\int_0^1 \xi F_\tau(1, 1+\alpha\xi)\,\mathrm{d}\xi \int_0^1 F_{p_e}(1, 1+\alpha\xi)\,\mathrm{d}\xi}{\displaystyle\int_0^1 F_\tau(1, 1+\alpha\xi)\,\mathrm{d}\xi}, \tag{5.8}$$

which provides a practical means of testing whether $Q_N > 0$ for a given rheology, and hence whether instability occurs at sufficiently small β. Many rheologies, including the power-law (2.4) and the exponential rheology used by Fowler (2000) are of the form

$$F(\tau, p_e) = f(\tau^b/p_e), \qquad b > 0 \text{ constant}, \qquad f'(\zeta) > 0 \text{ when } \zeta > 0. \tag{5.9}$$

For rheologies of this type, (5.8) takes the form

$$Q_N = \frac{\displaystyle\int_0^1 \xi^2 s(\xi)\,\mathrm{d}\xi \int_0^1 s(\xi)\,\mathrm{d}\xi - \left(\int_0^1 \xi s(\xi)\,\mathrm{d}\xi\right)^2}{\displaystyle\int_0^1 (1+\alpha\xi) s(\xi)\,\mathrm{d}\xi} \tag{5.10}$$

where $s(\xi) = (1+\alpha\xi)^{-2} f'(1/[1+\alpha\xi]) > 0$. It is straightforward to see then that $Q_N > 0$ follows by the Cauchy–Schwarz inequality applied to the product $\xi \times 1$ with weight function $s(\xi)$. More explicitly, the denominator in (5.10) is clearly positive, while the

numerator can be written as:

$$\int_0^1 \xi^2 s(\xi)\,\mathrm{d}\xi \int_0^1 s(\xi)\,\mathrm{d}\xi - \left(\int_0^1 \xi s(\xi)\,\mathrm{d}\xi\right)^2 = \frac{\displaystyle\int_0^1 \left[\left(\int_0^1 s(\xi')\,\mathrm{d}\xi'\xi - \int_0^1 \xi' s(\xi')\,\mathrm{d}\xi'\right)^2 s(\xi)\right]\mathrm{d}\xi}{\displaystyle\int_0^1 s(\xi'')\,\mathrm{d}\xi''}.$$

Clearly, this quantity is positive since $s(\xi)\geqslant 0$ for $0\leqslant\xi\leqslant 1$. Consequently, for rheologies of the type (5.9), we generally expect instability, at least at small β. Importantly, this result holds regardless of the values of the exponents m and n in (2.4) and therefore applies to the nearly plastic case of large $m\approx n$ (see also § 7).

We do not investigate the role of β in controlling bed stability in detail here, although the instability criterion (5.7) clearly indicates that instability requires β to be below a critical value $(\bar{U}_0 - Q_h)/Q_N$. This is not considered in more detail here because critical values of β for the power-law (2.4) have been calculated Schoof (2002, § 5.5.2), where it was found that in all physically realistic cases, β lies below the critical value and instability occurs.

6. A nonlinear model

Having established that the instability mechanism is feasible for a large class of rheologies, our next task is to study the nonlinear evolution of the ice–till interface. As the fastest growing wavevector has zero transverse component, we restrict ourselves to the two-dimensional case where $v\equiv 0$ and all variables are independent of the transverse coordinate y. We will also omit the superscripts $^{(0)}$ on h and q. Then the model in § 4.3 takes the form

$$\nabla^2\boldsymbol{u} - \nabla p = \boldsymbol{0}, \qquad \nabla\cdot\boldsymbol{u} = 0 \qquad \text{on } z>0,\ 0<x<a, \tag{6.1a, b}$$

$$\frac{\partial u}{\partial z} + \frac{\partial w}{\partial x} \to 0, \qquad p\to 0 \qquad \text{as } z\to\infty. \tag{6.2}$$

$$w = \bar{U}\frac{\partial h}{\partial x} - \frac{\partial q}{\partial x}, \qquad \tau_b = 1+\gamma\left(\frac{\partial u}{\partial z}+\frac{\partial w}{\partial x}\right), \qquad N = 1+\beta h + p - 2\frac{\partial w}{\partial z} \qquad \text{on } z=0, \tag{6.3a–c}$$

$$\tau_b = \tau(\bar{U}, N, h), \qquad q = Q(\bar{U}, N, h), \tag{6.4}$$

$$\frac{\partial h}{\partial t} + \frac{\partial q}{\partial x} = 0, \tag{6.5}$$

with periodic boundary conditons at $x=0, a$. The particular forms chosen for $\tau(\bar{U}, N, h)$ amd $Q(\bar{U}, N, h)$ are those which arise from the power-law (2.4), which reads $F(\tau, p_e) = \tau^m p_e^{-n}$ in dimensionless form. Integrating (4.5) and (4.6) explicitly, we obtain for $n\neq 1, 2$:

$$u_b(\tau_b, N, h) = \frac{\tau^m}{\alpha(n-1)N^{n-1}}\left[1 - \left(\frac{N}{N+\alpha(1+h)}\right)^{n-1}\right], \tag{6.6}$$

$$q_b(\tau_b, N, h) = \frac{\tau^m}{\alpha^2(n-1)(n-2)N^{n-2}}\left[1 - \frac{N+(n-1)\alpha(1+h)}{N}\left(\frac{N}{N+\alpha(1+h)}\right)^{n-1}\right], \tag{6.7}$$

which can be inverted to give

$$\tau(\bar{U}, N, h) = \bar{U}^{1/m} N^{(n-1)/m}[\alpha(n-1)]^{1/m}\left[1 - \left(\frac{N}{N+\alpha(1+h)}\right)^{n-1}\right]^{-1/m}, \tag{6.8}$$

$$Q(\bar{U}, N, h) = \frac{\bar{U}N}{\alpha(n-2)} - \frac{\bar{U}(n-1)(1+h)}{n-2}\left(\frac{N}{N+\alpha(1+h)}\right)^{n-1}\left[1 - \left(\frac{N}{N+\alpha(1+h)}\right)^{n-1}\right]^{-1}. \tag{6.9}$$

As a first step, we reduce the nonlinear boundary-value problem (6.1)–(6.4) to an integral equation over the lower boundary of the ice flow. The simplest way of doing so is to exploit the periodicity in x of the domain and introduce the discrete Fourier transform of a generic function $f(x, z, t)$ with period a as

$$\hat{f}_n(z, t) = \frac{1}{a}\int_0^a f(x, z, t)\exp(-\mathrm{i}k_n x)\,\mathrm{d}x, \tag{6.10}$$

where n is an integer and $k_n = 2\pi n/a$. In order to solve (6.1a, b), we introduce a stream-function ψ such that $\boldsymbol{u} = (\partial\psi/\partial z, -\partial\psi/\partial x)$, and (6.1$b$) is satisfied automatically. Solutions for ψ and p satisfying (6.2) can be written in the form

$$\hat{\psi}_n = (A_n z + B_n)\exp(-|k_n|z), \qquad \hat{p}_n = -\mathrm{i}2k_n A\exp(-|k_n|z), \tag{6.11}$$

where A_n and B_n are independent of z (but depend on t and n). Implementation of the boundary conditions (6.3a–c) for $n \neq 0$ then yields the relations

$$-\mathrm{i}k_n B_n = \mathrm{i}k_n(\bar{U}\hat{h}_n - \hat{q}_n), \qquad \hat{N}_n = \beta\hat{h}_n - 2\mathrm{i}k_n|k_n|B_n, \tag{6.12}$$

or equivalently

$$\hat{N}_n = \beta\hat{h}_n + 2\mathrm{i}|k_n|k_n(\bar{U}\hat{h}_n - \hat{q}_n), \qquad n \neq 0, \tag{6.13}$$

with $\hat{N}_0 = 1$. Note that the Fourier components of shear stress τ_b do not enter into this expression. Re-arranging, we are led to

$$\hat{q}_n - \bar{U}\hat{h}_n + \beta\frac{\mathrm{i}}{2|k_n|k_n}\hat{h}_n - \frac{\mathrm{i}}{2|k_n|k_n}\hat{N}_n = 0. \tag{6.14}$$

Next, we invert the relationship $q = Q(\bar{U}, N, h)$ to give $N = \tilde{N}(\bar{U}, q, h)$. This inversion is unique for q in the range of $Q(\bar{U}, \cdot, h)$ because $Q(\bar{U}, \cdot, h)$ in (6.9) is mononically increasing in N (this can be shown by analogy with the derivation of (5.10)); however, in general, the inversion is possible only numerically. A nonlinear integral equation of Hammerstein type (Rall 1969) for q is then obtained by taking the inverse of the discrete Fourier transform and applying the convolution theorem:

$$q(x, t) - \bar{q}(t) - \bar{U}(t)h(x, t) + \beta\int_0^a K(x-x')h(x', t)\,\mathrm{d}x' - \int_0^a K(x-x')N(x', t)\,\mathrm{d}x' = 0, \tag{6.15}$$

where $N(x',t)=\tilde{N}(\bar{U}(t),q(x',t),h(x',t))$, while $\bar{q}(t)=\hat{q}_0(t)=a^{-1}\int_0^a q(x,t)\,\mathrm{d}x$ is the mean value of till flux, and the kernel K is given by

$$K(x)=\sum_{n=-\infty,\,n\neq 0}^{\infty}\frac{\mathrm{i}\exp(\mathrm{i}k_n x)}{2|k_n|k_n a}. \tag{6.16}$$

For an alternative, more elegant derivation of (6.15) using complex variables, see Schoof (2002). It remains to fix the two spatially constant terms $\bar{U}(t)$ and $\bar{q}(t)$. One constraint is provided by the horizontal force balance relation (4.19), which we cast as

$$\int_0^a \tilde{\tau}(\bar{U}(t),q(x,t),h(x,t))-1\,\mathrm{d}x=0, \tag{6.17}$$

where $\tilde{\tau}(\bar{U},q,h)$ is obtained from $\tau(\bar{U},N,h)$ by substituting $N=\tilde{N}(\bar{U},q,h)$. Another constraint arises from a two-dimensional equivalent of the vertical force balance condition (4.15*b*):

$$\int_0^a \tilde{N}(\bar{U}(t),q(x,t),h(x,t))-1\,\mathrm{d}x=0. \tag{6.18}$$

Given bed topography $h(x,t)$ at fixed t, equations (6.15)–(6.18) are sufficient to calculate flux and sliding velocity, for which Schoof (2002) presents a numerical scheme based on a Newton–Kantorovič iteration. Meanwhile, the evolution of the ice–till interface is governed by

$$\frac{\partial h}{\partial t}+\frac{\partial q}{\partial x}=0. \tag{6.19}$$

Here we use a Fourier collocation scheme with a fully implicit time step (e.g. Trefethen 2000) to solve (6.15)–(6.19) with $\tilde{N}$ and $\tilde{\tau}$ defined by the power law (2.4).

A typical result is displayed in figure 3. As expected, small perturbations on the bed grow, but importantly the growth is not bounded. In fact, the solution procedure was terminated when N reached zero on the downstream side of the largest bed bump (figure 4). Zero interfacial effective pressure physically corresponds to compressive normal stress at the interface equalling water pressure; this is the point at which ice loses contact with the bed and a water-filled cavity forms in the lee of the bed bump, again a familiar phenomenon from glaciers sliding over undeformable beds (e.g. Fowler 1986; Schoof 2005). This outcome was encountered in all simulations carried out using a wide range of parameters α, β, m and n for which instability was predicted. It therefore appears that the nonlinearity present in the functions $\tilde{N}$ and $\tilde{\tau}$ (or Q and τ) is insufficient to cause bounded growth before the onset of cavitation. This conjecture will be supported further in the next section, where we show that taking the plastic limit $m\approx n\gg 1$ in the power law rheology (2.4) leads to an effective linearization of the model, and that unbounded growth must then be expected at least before the onset of cavitation.

These results suggest that an additional nonlinearity must be introduced into the model if bounded growth is to occur. In a separate paper, we show that a modification of the present model which takes account of cavitation allows for travelling-wave solutions, suggesting that the nonlinearity introduced by cavitation is sufficient to quench the instability.

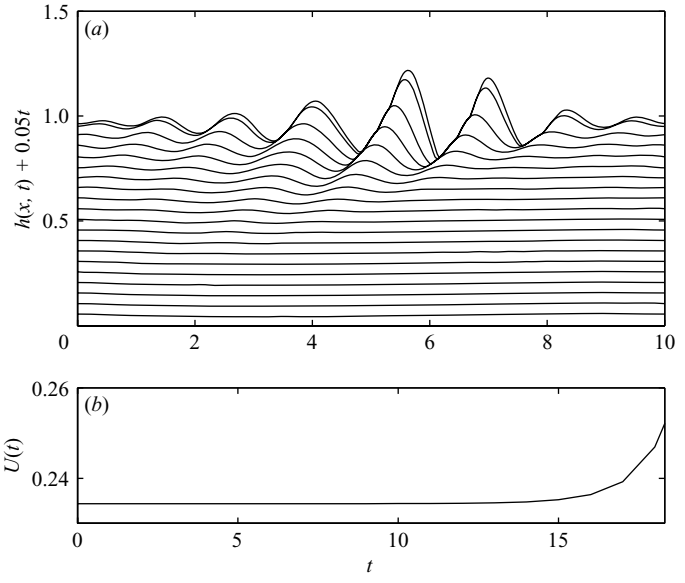

FIGURE 3. Nonlinear evolution of the ice–till interface with $m = n = 5$, $\alpha = 1$, $\beta = 0.1$ and $a = 10$ (recall that m and n are rheological parameters, while α measures the hydrostatic increase in effective pressure over the thickness of the sediment layer compared with mean interfacial effective pressure, while β depends on the difference between water and ice viscosities). (a) Solutions for $s(x, t)$ at unit time intervals are plotted with a vertical stagger for ease of viewing. The final bed shape at cavitation corresponds to $t = 18.3$. (b) The evolution of sliding velocity $\bar{U}(t)$ with time. The ice velocity increases as bed bumps grow. This is because sliding velocity is determined by till deformation through (4.19) rather than by drag due to bed bumps acting as obstacles to flow (which appears as a higher order term in force balance).

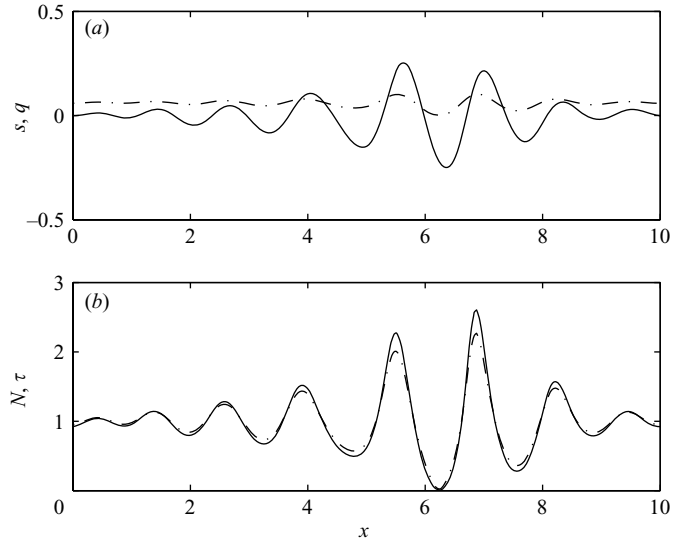

FIGURE 4. (a) Bed elevation s (solid line) and flux q (dot-dashed line) at the final time step of the simulation shown in figure 3. Clearly, q is largest on the upstream sides of bed bumps, showing that the bumps are still growing. (b) Effective pressure N (solid line) and shear stress τ_b (dot-dashed line) for the bed shown in (a). Both reach zero at $x = 6.3$, in the lee of the largest bed bump (ice flow is from left to right). When effective pressure reaches zero, ice lifts off the bed and a water-filled cavity forms.

7. 'Nearly plastic' rheologies

In this section, we consider briefly what happens in the limit of large $m \approx n$ in the model (6.1)–(6.8). The motivation for considering this limit is that it conforms most closely to what is observed in laboratory tests of till shearing. Before we proceed, we should point out that the model (6.1)–(6.8) itself was based on the asymptotic limit $\nu \ll 1$. If we consider the limit $m \approx n \gg 1$ in the confines of this model, rather than returning to the full problem (2.1)–(2.13), we are restricting ourselves to a case in which limits in ν are taken first (since the relevant limits in ν and n may not commute). Technically (though we will not explore this further here), this implies that $\nu \ll 1/\sqrt{n} \ll 1$.

Consider then (6.9), and suppose that N remains uniformly bounded, while $1+h > 0$ everywhere uniformly, so there is no sediment pinch-out. Then $N/(N + \alpha(1 + h)) \leqslant M < 1$ for some fixed positive M. Then $Q(\bar{U}, N, h)$ behaves as (see also Schoof 2002, chap. 6)

$$Q(\bar{U}, N, h) \sim \frac{\bar{U} N}{\alpha(n-2)} + O(nM^n), \tag{7.1}$$

and the correction tends to zero as $n \to \infty$ faster than the first term does (as $nM^n = o(n^{-1})$ for $M < 1$ and $n \to \infty$). Hence, for large n, we can approximate $Q \sim \bar{U}N/(\alpha(n-2))$ and Q is linear in N. Unbounded growth before cavitaton is now unsurprising, as the only nonlinearity present resides in the fact that Q also depends on the (spatially constant) velocity $\bar{U}$, which is determined by the shear stress function $\tau(\bar{U}, N, h)$ through (6.17).

For the special case of $m = n - 1$, this argument can be taken a step further: if we consider (6.8), we see similarly that

$$\tau(\bar{U}, N, h) \sim [\alpha(n-1)\bar{U}]^{1/m} N^{(n-1)/m} (1 - O(M^{n-1}))^{-1/m}, \tag{7.2}$$

and hence $\tau \sim [\alpha(n-1)\bar{U}]^{1/m} N^{(n-1)/m}$. For $m = n-1$, this gives $\tau \sim [\alpha m \bar{U}]^{1/m} N$, and (6.17) is simply

$$[\alpha m \bar{U}(t)]^{1/m} \frac{1}{a} \int_0^a N(x,t)\, \mathrm{d}x = 1, \tag{7.3}$$

since $\bar{U}$ is independent of position. From (6.15), we know that $a^{-1} \int_0^a N(x,t)\,\mathrm{d}x = 1$, and $\bar{U}$ is in fact constant in time as well as space:

$$\bar{U} = \frac{1}{\alpha m}, \tag{7.4}$$

and the model is fully linear: we have (6.1)–(6.5) with τ and Q given by

$$\tau = [\alpha m \bar{U}]^{-1/m} N^{(n-1)/m} = N, \qquad Q = \frac{\bar{U} N}{\alpha(n-2)} = \frac{N}{\alpha^2(n-1)(n-1)}, \tag{7.5}$$

and $\bar{U}$ given by (7.4). The linearity of this model implies that, if growth occurs, it must be unbounded – until the onset of cavitation.

More generally, we can argue that for large $m \approx n$, the outer flow problem which describes the ice sheet as a whole is unlikely to be a classical lubrication flow and hence that the far-field boundary conditions (2.13) ought to be revisited. Suppose that the outer flow of the ice sheet is not a lubrication flow but, for instance, behaves similarly to a viscous membrane, as is the case for ice streams and ice shelves (see e.g. MacAyeal 1989; Schoof 2006*a*). In that case, neither shear stress nor sliding velocity at the base of the outer flow (corresponding to the matching region with the inner

flow considered here) can necessarily be prescribed independently, but are related through the solution of the outer flow.

Clearly, the far-field shear stress $\bar{\tau}\boldsymbol{i}$ in the boundary layer can be identified with the basal shear stress in the outer flow, where we have assumed in the set-up of the problem that the x-axis is, at least on the inner length scale $[x]$, aligned with the direction of basal shear stess in the outer flow. The only change from the original set-up of the problem is now that we may not necessarily prescribe $\bar{\tau}$. Meanwhile, from (3.8a) we find that $\boldsymbol{u}=[u](\boldsymbol{u}^\star+\nu\gamma^{-1}z^\star\boldsymbol{i})=[u](\bar{U}\boldsymbol{i}+\nu\boldsymbol{u}^{(1)}+\nu\gamma^{-1}z^\star\boldsymbol{i}+O(\nu^2))$ in dimensional terms, where we have reintroduced the asterisk on $\boldsymbol{u}^\star$ to distinguish it from the dimensional velocity field $\boldsymbol{u}$. Hence, if the matching region between inner and outer flow is identified with $1\ll z^\star\ll\gamma\nu^{-1}$, then it is clear that $u_s\boldsymbol{i}=[u]\bar{U}\boldsymbol{i}$ is the dimensional basal velocity in the outer flow (see also Fowler 1981).

For the outer problem, the boundary-layer problem must specify a friction law, or specifically, a relationship between u_s, $\bar{\tau}$ and mean effective pressure $[N]=\rho gH-p_c$ (see also Schoof 2005). This is precisely what (6.17) provides. For $m\approx n\gg 1$, (7.2) can be used to cast (6.17) in dimensional terms – by redimensionalising all quantities involved – as

$$[K(n-1)(1-\phi)(\rho_s-\rho_w)u_s]^{1/m}\,(\rho gH-p_c)^{(n-1)/m}\left(\frac{1}{a}\int_0^a N^{(n-1)/m}\,\mathrm{d}x\right)=\bar{\tau}, \quad (7.6)$$

where $\rho gH-p_c=[N]$ is mean effective pressure, and K is the constant in (2.4). Approximating

$$\frac{1}{a}\int_0^a N^{(n-1)/m}\,\mathrm{d}x\approx\frac{1}{a}\int_0^a N\,\mathrm{d}x=1 \quad (7.7)$$

for $m\approx n\gg 1$ and using (6.15), we have

$$\bar{\tau}=\left[(n-1)K\frac{(1-\phi)(\rho_s-\rho_w)g}{\rho gH-p_c}u_s\right]^{1/m}(\rho gH-p_c)^{n/m}. \quad (7.8)$$

As $m\gg 1$ and $n/m\approx 1$, this states that dimensional far-field shear stress is only weakly dependent on the sliding velocity u_s, and approximately linear in mean effective pressure $\rho gH-p_c$. In other words, we have a regularized Coulomb friction law.

The mechanics of ice-sheet flow subject to a Coulomb friciton law have been explored in Schoof (2004, 2006a, b). Here, it suffices to note that the relevant solution procedure calculates velocity u_s at the base of the outer flow based on the basal yield stress distribution (which may, in those regions where sliding occurs, be identified with the basal shear stress). Thus, for a highly nonlinear till rheology (2.4) with large $m\approx n$, it makes more sense to impose the sliding velocity $u_s=[u]\bar{U}$ than the far-field shear stress $\bar{\tau}$ (as the latter is effectively controlled by mean effective pressure $\rho gH-p_c$). By an appropriate choice of scaling, we can then set $\bar{U}=1$. Equation (7.1) still provides till flux q as $q=\bar{U}N/[\alpha(n-2)]=N/[\alpha(n-2)]$, while shear stress τ_b can be calculated from (7.2) as $\tau_b=N$, where with $\bar{U}=1$ fixed we can now legitimately approximate $[\alpha(n-1)\bar{U}]^{1/m}\sim 1$. The appropriate model in two dimensions is then

$$\nabla^2\boldsymbol{u}-\nabla p=\boldsymbol{0}, \qquad \nabla\cdot\boldsymbol{u}=0 \qquad \text{on } z>0, \quad (7.9)$$

$$\frac{\partial u}{\partial z}+\frac{\partial w}{\partial x}\to 0, \qquad p\to 0 \qquad \text{as } y\to 0, \quad (7.10)$$

$$w=\frac{\partial h}{\partial x}-\frac{\partial q}{\partial x}, \qquad \tau_b=1+\gamma\left(\frac{\partial u}{\partial z}+\frac{\partial w}{\partial x}\right), \qquad N=1+\beta h+p-2\frac{\partial w}{\partial x}, \quad \text{on } z=0, \quad (7.11a\text{–}c)$$

$$\frac{\partial h}{\partial t} + \frac{\partial q}{\partial x} = 0, \tag{7.12}$$

$$q = \frac{N}{\alpha(n-2)}, \qquad \tau_b = N. \tag{7.13a, b}$$

As a final point, we may note that the flux in (7.13) is small for large n. An $O(1)$ flux can be recovered under the rescaling

$$q^{\star\star} = \alpha n q, \qquad h^{\star\star} = \alpha n h, \qquad x^{\star\star} = \sqrt{\alpha n}\, x, \qquad t^{\star\star} = \sqrt{\alpha n}\, t, \qquad \boldsymbol{u}^{\star\star} = \sqrt{\alpha n}\, \boldsymbol{u}. \tag{7.14}$$

A more in-depth physical interpretation of this rescaling may be found in Schoof (2002, chap. 6). Here we note only that (7.13) suggests that, for large n, till deformation is restricted to a thin layer close to the ice–till interface, of thickness $\sim 1/(\alpha n)$ in units of $[z]$ as defined in § 3; hence, identifying the vertical scale $[z]$ with d is inappropriate for highly nonlinear rheologies. The rescaling defines a new scale for the size of bed bumps, equal to the effective thickness of deforming sediment:

$$[z]^{\star\star} = [h]^{\star\star} = \frac{d}{\alpha n} = \frac{[N]}{n(1-\phi)(\rho_s - \rho_w)g}, \tag{7.15}$$

which is independent of available sediment thickness and depends only on effective pressure and material parameters. Correspondingly, the relevant wavelength scale is, in terms of velocity and material parameters

$$[x]^{\star\star} = \frac{[x]}{\sqrt{n\alpha}} = \sqrt{\frac{\eta[u]}{n(1-\phi)(\rho_s - \rho_w)g}}. \tag{7.16}$$

Dropping the asterisks on the double-starred dimensionless variables, the model (7.9)–(7.13) then remains unchanged under this rescaling except that (7.11c) and (7.13a) may be rewritten at leading order in $(\alpha n)^{-1}$ as

$$N = 1 + p - 2\frac{\partial w}{\partial x}, \qquad q = N. \tag{7.17}$$

The resulting model is clearly linear, and the flat-bed solution $h \equiv 0$ can easily be shown to be unstable: in the notation of § 5, we have $Q_N = 1 > 0$ and $\beta = 0$, and the model admits Fourier mode solutions of the form $h(x,t) = \mathrm{Re}(\exp(\mathrm{i}kx + \sigma t))$, with $\sigma = 2|k|^3/(1 + 2\mathrm{i}k|k|)$. The linearity moreover allows the case of cavitation to be treated more easily, as we will explore in a separate paper.

8. Discussion

In this paper, we have presented a detailed study of an instability in coupled ice–sediment flow, modelled as the slow flow of a Newtonian medium over a thin layer of viscous material with a pressure-dependent viscosity. As was shown in § 5, the basic mechanism relies on a sediment flux which increases (as a result of pressure-dependent viscosity) when compressive normal stress at the ice–sediment interface is raised while the horizontal component of velocity of the interface remains constant. Under these circumstances, the higher compressive normal stress typically exerted by moving ice on the upstream side of a bed bump compared with the downstream side corresponds to a higher till flux going into the bed bump than out of it, and the bump grows. It was shown that this behaviour is expected for a class of simple effective-pressure dependent viscous rheologies, including highly nonlinear 'nearly plastic' ones. Dimensionally, we

see from (7.15) and (7.16) that the expected size of bed bumps increases with effective pressure – where we require the additional caveat that at very high effective pressures, the sediment may not deform at all, an effect which can be represented through incorporation of a yield stress in the model (e.g. Boulton & Hindmarsh 1987) – while the instability length scale increases as the square root of velocity.

With regard to the glaciological debate about till rheology, our results suggest the following: Hindmarsh and Fowler's instability does not so much depend on a viscous rheology for till as on the ability to parameterize till flux in terms of effective pressure and till surface velocity such that till flux increases with effective pressure at constant till surface velocity. It is conceivable that the latter is possible even if shear stress at the surface of the till must always attain a prescribed value, as would be expected for a plastic till.

The growth of instability was also shown to be unbounded until the onset of cavity formation, which occurs when compressive normal stress in the lee of a bump on the ice–sediment interface drops to the local porefluid pressure. Preliminary results to be reported in separate paper (see also Schoof 2002, chap. 6) indicate that cavity formation allows at least for the formation of travelling waves, and may therefore be sufficient to stop the growth of the instability.

The intention of the original proponents of the instability mechanism had been to describe the formation of a type of subglacial landforms known as drumlins. For a number of reasons, our results do not support this notion. First, our stability analysis has indicated that the fastest growing Fourier mode corresponds to roll waves with infinite transverse wavelengths, and there is no obvious mechanism in the model for symmetry breaking which could allow for the formation of three-dimensional bedforms such as drumlins (see figure 1), though the model could conceivably account for ridges or 'Rogen moraines' transverse to the ice flow direction (e.g. Aario 1987). Furthermore, geological evidence shows that the cores of drumlins often consist of undeformed stratified sediment (Alden 1905; Sharpe 1987), which sometimes shows evidence of having been deposited in a non-glacial environment (Schaeffer 1969; Goldthwait 1974). By contrast, the instabilities predicted by our model appear to be advected downstream and, at least at cavitation, the amplitude of bed undulations scales with the thickness $[z]$ of the deforming layer. It is therefore difficult to conceive of the bed undulations predicted by our model as preserving sedimentary structures in a subglacial till layer, as this would require a thin deforming layer atop an essentially stationary bedform of much larger amplitude than the deforming layer. A third consideration is the height of drumlins. Typical estimates of the depth to which subglacial sediments deform range from a few centimetres (Engelhardt & Kamb 1998) to around a metre (Boulton & Hindmarsh 1987). If the amplitude scale for evolved bed undulations is the same as the scale for the thickness of till which is effectively deforming (and we are not able to demonstrate this conclusively here as we cannot follow the evolution of the bed beyond cavitation, but see also Schoof 2002, chap. 6), then our model seems unable to predict bed bumps more than a few metres high. This is hardly adequate to explain the formation of drumlins, which are often tens of metres high.

The fact that the model predicts the spontaneous formation of cavities on deformable glacier beds is possibly of much greater practical interest than the tenuous link between the model and the origin of drumlins. The formation of a network of subglacial cavities which are capable of storing large quantites of slow-flowing water has been linked with the surging behaviour of some temperate glaciers, in particular the well-studied Variegated Glacier in Alaska (Fowler 1987; Kamb 1987). However,

models which attempt to describe the formation of subglacial cavities generally rely on the assumption of an undeformable bed (Fowler 1986; Kamb 1987; Schoof 2005), whereas it is known that the Variegated Glacier is underlain by till (Harrison, Kamb & Engelhardt 1986). Our model provides a possible theoretical explanation for the existence of a linked cavity network at the base of a soft-bedded glacier. As our work in §§ 5 and 7 shows, this conclusion seems to be robust when considering highly non-linear nearly plastic rheologies, at least when these are of power-law type.

This work was supported by the US National Science Foundation under grant no. DMS-03227943, and by an EPSRC doctoral studentship at the Mathematical Institute, Oxford University. I should like to thank the editor, Howard Stone, as well as Richard Hindmarsh and two anonymous referees for their thorough scrutiny.

Appendix. The thermodynamic basis for effective-pressure-dependent viscosity

Dell'Isola & Hutter (1998) construct a thermodynamics-based mixture theory for till deformation in which porosity ϕ (or $1-\nu$ in their notation, where ν is the solid volume fraction) controls sediment viscosity; in addition, they use only a single pressure variable, denoted below by P (to avoid confusion with our p). At constant temperature, stress $\boldsymbol{T}_s$ supported by the till is written as (dell's Isola & Hutter's equation (2.12)):

$$\boldsymbol{T}_s = -(1-\phi)(\beta_s(\phi) + P)\boldsymbol{I} + \boldsymbol{t}_s \tag{A 1}$$

where the thermodynamic pressure β_s is determined as a function of ϕ by the Helmholtz free energy of the till-water mixture, $\boldsymbol{I}$ is the identity tensor (whose components are given by the Kronecker delta), and $\boldsymbol{t}_s$ is a deviatoric stress defined implicitly by

$$\boldsymbol{D} - \tfrac{1}{3}\mathrm{Tr}(\boldsymbol{D})\boldsymbol{I} = A(\phi, t_s)\boldsymbol{t}_s, \tag{A 2}$$

where A is fluidity, t_s the second invariant of $\boldsymbol{t}_s$, and $\mathrm{Tr}(\boldsymbol{D})$ denotes the trace of the sediment strain rate tensor $\boldsymbol{D}$. Under the assumption made in the present paper that porefluid does not support significant shear stresses, the stress supported by the fluid may be written as

$$\boldsymbol{T}_f = -\phi P\boldsymbol{I}, \tag{A 3}$$

which amounts to setting dell'Isola & Hutter's fluid viscosities μ_f and λ_f to zero. For slow flow, momentum conservation in dell'Isola & Hutter's theory becomes

$$\nabla\cdot\boldsymbol{T}_s - (1-\phi)\rho_s g\boldsymbol{k} + \boldsymbol{m} = \boldsymbol{0}, \qquad \nabla\cdot\boldsymbol{T}_f - \phi\rho_w g\boldsymbol{k} - \boldsymbol{m} = \boldsymbol{0}, \tag{A.4a, b}$$

where the non-equilibrium part of the interaction term $\boldsymbol{m}$ describes a Darcy force:

$$\boldsymbol{m} = -\{P + (1-\rho_s)/[(1-\phi)\rho_s + \phi\rho_w])\beta_s\}\nabla\phi + \boldsymbol{q}_w/\kappa, \tag{A.5}$$

where $\kappa(\phi)$ is a permeability and $\boldsymbol{q}_w$ is water flux relative to the till matrix (porosity multiplied by water velocity relative to the matrix velocity $\boldsymbol{u}$).

To arrive at an effective-pressure based description, define total pressure p and liquid pressure p_w by

$$p = (1-\phi)\beta_s(\phi) + P, \qquad p_w = P. \tag{A.6}$$

If we define the usual effective pressure as $p_e = p - p_w$, we find

$$p_e = (1-\phi)\beta_s(\phi) \doteq f(\phi). \tag{A.7}$$

If $f(\phi)$ thus defined is monotonically decreasing, then ϕ can be written as a function of p_e, and we can legitimately express till viscosity as a function of p_e in (A 2). If, in addition, the modulus of the first derivative f' of f is sufficiently large, then it is clear that for a limited range of values of p and p_w, and hence of p, variations in porosity ϕ about some mean value ϕ_0 will be small. Indeed, approximating $p_e - p_{e,0} = f(\phi) - f(\phi_0) \approx f'(\phi_0)(\phi - \phi_0)$ where $f(\phi_0) = p_{e,0}$ is a reference effective pressure, it is clear that $-1/f'(\phi_0)$ plays the role of a compressibility, which is small when f' is large. This allows us to approximate the till matrix as incompressible, hence (2.5*b*) holds and $\mathrm{Tr}(\boldsymbol{D}) = 0$ in (A 2). Nonetheless, it is conceivable that small changes in ϕ still lead to large changes in sediment viscosity through a sensitive dependence of $A(\phi, t_s)$ on ϕ, and a dependence of viscosity on effective pressure is retained. On the other hand, we can approximate porosity gradients to zero, notably in (A.5). Equation (A 4*b*) thus gives an ordinary Darcy's law for water flux:

$$\boldsymbol{q}_w \approx -\phi_0 \kappa(\phi_0) \nabla p_w - \phi_0 \rho_w g \boldsymbol{k}. \tag{A.8}$$

For a fixed water flux and sufficiently large permeability, we find that p_w changes hydrostatically, as in Fowler and Hindmarsh's model (equation (2.6) in this paper). Similarly, adding (A 4*a*) and (A 4*b*) yields

$$-\nabla p + \nabla \cdot \boldsymbol{t}_s - [(1 - \phi_0)\rho_s + \phi_0 \rho_w] g \boldsymbol{k} = \boldsymbol{0}, \tag{A.9}$$

which we may identify with (2.5*a*) if we put $F(\tau, p_e) = A(\phi_0 + [p_e - p_{e,0}]/f'(\phi_0), \tau))\tau$, remembering that $\mathrm{Tr}(\boldsymbol{t}_s) \approx 0$ owing to the approximate incompressibility of the till matrix.

It remains to point out that our prescription of stress continuity at the ice–till interface differs from that of dell'Isola & Hutter. Specifically, by imposing a stress on the ice side of the interface, dell'Isola & Hutter's approach (postulate 3.1 of their paper) yields both fluid and solid stresses on the till side. Hence, when the till flows in simple shear, effective pressure at the interface is prescribed in dell'Isola & Hutter's model by normal stress and is not affected by the presence of a drainage system. In our approach, fluid stress is prescribed by other means – specifically by a drainage system – the difference between the models presumably being accounted for by different constitutive relations for these interface stresses.

REFERENCES

Aario, R. 1987 Drumlins of Kuusamo and Rogen-ridges of Ranua, northeast Finland. In *Drumlin Symposium* (ed. J. Menzies & J. Rose), pp. 87–102. Balkema, Rotterdam.

Alden, W. C. 1905 The drumlins of southeastern Wisconsin. *US Geol. Surv. Bull.* B **76**, 9–46.

Alley, R. B. & Bindschadler, R. A. (ed.) 2001 *The West Antarctic Ice Sheet: Behaviour and Environment*. Washington, DC. American Geophysical Union.

Balmforth, N. J., Craster, R. V. & Toniolo, C. 2003 Interface instability in non-Newtonian fluid layers. *Phys. Fluids* **15** (11), 3370–3384.

Blankenship, D. D., Bentley, C. R., Rooney, S. T. & Alley, R. B. 1986 Seismic measurements reveal a saturated porous layer beneath an active antarctic ice stream. *Nature* **322**, 54–57.

Boulton, G. S. & Dobbie, K. E. 1998 Slow flow of granular aggregates: the deformation of sediments beneath glaciers. *Phil. Trans. R. Soc. Lond* A **356** (1747), 2713–2745.

Boulton, G. S. & Hindmarsh, R. C. A. 1987 Sediment deformation beneath glaciers: rheology and geological consequences. *J. Geophys. Res.* **92** (B9), 9059–9082.

Engelhardt, H. & Kamb, B. 1997 Basal hydraulic system of a West Antarctic ice stream: constraints from borehole observations. *J. Glaciol.* **43**, 207–230.

Engelhardt, H. & Kamb, B. 1998 Basal sliding of Ice Stream B. *J. Glaciol.* **44**, 223–230.

Fowler, A. C. 1981 A theoretical treatment of the sliding of glaciers in the absence of cavitation. *Phil. Trans. R. Soc. Lond.* **298** (1445), 637–685.

Fowler, A. C. 1986 A sliding law for glaciers of constant viscosity in the presence of subglacial cavitation. *Proc. R. Soc. Lond* A. **407**, 147–170.

Fowler, A. C. 1987 Sliding with cavity formation. *J. Glaciol.* **33** (105), 255–267.

Fowler, A. C. 1989 A mathematical analysis of glacier surges. *SIAM J. Appl. Maths* **49**, 246–263.

Fowler, A. C. 2000 An instability mechanism for drumlin formation. In *Deformation of Glacial Materials* (ed. A. Maltman, M. J. Hambrey & B. Hubbard), *Spec. Pub. Geol. Soc.*, vol. 176, pp. 307–319. The Geological Society London.

Fowler, A. C. 2001 Dunes and drumlins. In *Geomorphological Fluid Mechanics* (ed. N. J. Balmforth & A. Provenzale), *Lecture Notes in Physics*, vol. 582, pp. 430–454. Springer.

Fowler, A. C. 2002 Rheology of subglacial till (correspondence). *J. Glaciol.* **48** (163), 631–632.

Fowler, A. C. 2003 On the rheology of till. *Ann. Glaciol.* **37**, 55–59.

Fowler, A. C. & Larson, D. A. 1978 On the flow of polythermal glaciers. I. Model and preliminary analysis. *Proc. R. Soc. Lond.* A **363**, 217–242.

Goldthwait, R. P. 1974 Rates of formation of glacial features in Glacier Bay, Alaska. In *Glacial Geomorphology* (ed. D. R. Coates), *Binghampton Symposia in Geomorphology*, vol. 5, chap. 6, pp. 163–185. Allen & Unwin.

Greenberg, J. M. & Shyong, W. 1990 Surging glacial flows. *IMA J. Appl. Maths* **45** (3), 195–223.

Harrison, W. D., Kamb, B. & Engelhardt, H. 1986 Morphology and motion at the bed of a surge-type glacier. *ETH Zürich Versuchanst. Wasserbau Hydrol. Glaziol. Mitt.* **90**, 55–56.

Hindmarsh, R. C. A. 1998 The stability of a viscous till sheet coupled with ice flow, considered at wavelengths less than the ice thickness. *J. Glaciol.* **44** (146), 285–292.

dell'Isola, F. & Hutter, K. 1998 What are the dominant thermomechanical processes in the basal sediment layer of large ice sheets? *Proc. R. Soc. Lond.* A **454**, 1169–1195.

Iverson, N. R., Baker, R. W., Hooke, R. LeB., Hanson, B. & Jansson, P. 1999 Coupling between a glacier and a soft bed: I. A relation between effective pressure and local shear stress determined from till elasticity. *J. Glaciol.* **45** (149), 31–40.

Iverson, N. R. & Iverson, R. M. 2001 Distributed shear of subglacial till due to Coulomb slip. *J. Glaciol.* **47** (158), 481–488.

Kamb, B. 1970 Sliding motion of glaciers: theory and observation. *Rev. Geophys.* **8**, 673–728.

Kamb, B. 1987 Glacier surge mechanism based on linked cavity configuration of the basal water conduit system. *J. Geophys. Res.* **92** (B9), 9083–9100.

Kamb, B. 1991 Rheological nonlinearity and flow instability in the deforming bed mechanism of ice stream motion. *J. Geophys. Res.* **96** (B10), 16 585–16 595.

Kamb, B. 2001 Basal zone of the West Antarctic ice streams and its role in lubrication of their rapid motion. In *The West Antarctic Ice Sheet: Behaviour and Environment* (ed. R. B. Alley & R. A. Binschadler), pp. 157–199. American Geophysical Union.

Kao, T. W. 1968 Role of viscosity stratification in the stability of two-layer flow down an inclined plane. *J. Fluid Mech.* **33**, 561–572.

MacAyeal, D. R. 1989 Large-scale flow over a viscous basal sediment: theory and application to Ice Stream E, Antarctica. *J. Geophys. Res.* **94** (B4), 4017–4087.

Morland, L. W. & Johnson, I. R. 1980 Steady motion of ice sheets. *J. Glaciol.* **25** (92), 229–246.

Ng, F. S. L. 1998 Mathematical modelling of subglacial drainage and erosion. DPhil thesis, Oxford University. *http://www.maths.ox.ac.uk/research/theses/*.

Nye, J. F. 1969 A calculation of the sliding of ice over a wavy surface using a Newtonian viscous approximation. *Proc. R. Soc. Lond.* A **311**, 445–467.

Paterson, W. S. B. 1994 *The Physics of Glaciers*, 3rd edn. Pergamon.

Rall, L. B. 1969 *Computational Solution of Nonlinear Operator Equations*. J. Wiley.

Schaeffer, I. 1969 Der Drumlin von Hörmatting in Oberbayern. *Eiszeitalter u. Gegenw.* **20**, 175–195.

Schoof, C. 2002 Mathematical models of glacier sliding and drumlin formation. DPhil thesis, Oxford University. *http://www.maths.ox.ac.uk/research/theses/*.

Schoof, C. 2004 On the mechanics of ice stream shear margins. *J. Glaciol.* **50** (169), 208–218.

Schoof, C. 2005 The effect of cavitation on glacier sliding. *Proc. R. Soc. Lond.* A **461**, 609–627. doi:10.1098/rspa.2004.1350.

Schoof, C. 2006*a* A variational approach to ice-stream flow. *J. Fluid Mech.* **556**, 227–251.

Schoof, C. 2006*b* Variational methods for glacier flow over plastic till. *J. Fluid Mech.* **555**, 299–320.

Sharpe, D. S. 1987 The stratified nature of drumlins from Victoria Island and southern Ontario, Canada. In *Drumlin Symposium* (ed. J. Menzies & J. Rose), pp. 185–214. Balkema, Rotterdam.

Trefethen, L.N. 2000 *Spectral Methods in MATLAB*. SIAM.

Tulaczyk, S. 1999 Ice sliding over weak, fine-grained till: dependence of ice–till interactions on till granulometry. *Spec. Paper Geol. Soc. Am.* **337**, 159–177.

Tulaczyk, S., Kamb, W. B. & Engelhardt, H. F. 2000 Basal mechanisms of Ice Stream B, West Antarctica: 1. till mechanics. *J. Geophys. Res.* **105** (B1), 463–481.

Walder, J. S. & Fowler, A. C. 1994 Channelised subglacial drainage over a deformable bed. *J. Glaciol.* **40** (134), 3–15.